Power uprates
and plant life extension

CASL-U-2011-0075-000

Consortium for Advanced Simulation of LWRs

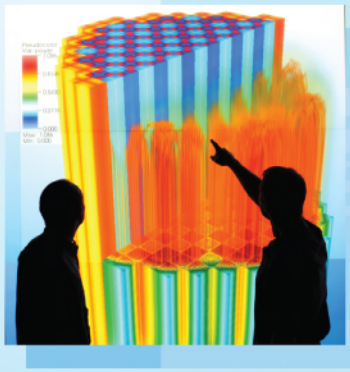

Engineering design
and analysis

L2:RTM.P2.01

Milestone Report and Completion Memo

Science-enabling
high performance
computing

Thomas Downar, RTM/University of Michigan
Brendan Kochunas, RTM/University of Michigan
Robert Brewster, CD-adapco
Emilio Baglietto, THM/CD-adapco

June 30, 2011

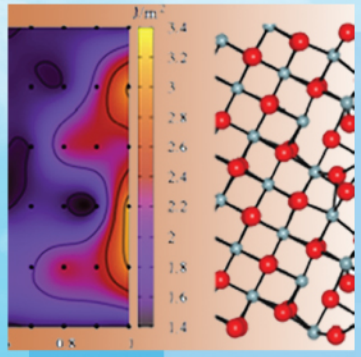

Fundamental science

Plant operational data

U.S. DEPARTMENT OF ENERGY | Nuclear Energy

Consortium for Advanced Simulation of LWRs

Consortium for Advanced Simulation of Light Water Reactors
Bldg. 2040, Room E-170, MS 6290
P.O. Box 2008
Oak Ridge, TN 37831-6290
Email: casl-info@ornl.gov

Date: 6/30/2011

To: Doug Kothe, CASL Director
Ronaldo Szilard, CASL Deputy Director
Gil Weigand, CASL Startup Manager
Paul Turinsky, CASL Chief Scientist
Mario Carelli, CASL Chief Strategy Officer
Jeff Banta, CASL Program Manager

c: Bill Martin, CASL RTM Lead
John Turner, CASL VRI Lead
Rob Lowrie, CASL THM Lead
Jess Gehin, CASL AMA Lead
Rod Schmidt, CASL VRI-PSS Project Lead
Andrew Godfrey, CASL AMA Staff
Scott Palmtag, CASL AMA Staff

From: Thomas Downar, RTM/University of Michigan
Brendan Kochunas, RTM/University of Michigan
Robert Brewster, CD-adapco
Emilio Baglietto, THM/CD-adapco

Level 2 Milestone Deliverable - RTM.P2.01

Milestone Due Date: 06/30/11

Milestone Completion Date:06/30/11

Description of Milestone:

This milestone marks the delivery of the capability to perform a 3D, full-core neutron transport (2D MOC + 1D diffusion) calculation coupled with single phase CFD T/H. The fuel pin powers and temperatures will be resolved radially, azimuthally, and axially. The DeCART code will be the transport solver and Star-CCM+ will be the T-H solver. The coupling will be performed explicitly via file I/O (loose coupling) between DeCART and Star-CCM+, and coupling iterations will be performed until convergence is achieved, where convergence is measured by appropriate norms in both DeCART and Star-CCM+. Quarter-core symmetry may be used for the demonstration calculation but the capability to analyze a full-core configuration without taking advantage of symmetry is required.

Completion Proof of the Milestone:

This document and the attached report [1] serve as proof of completion of this milestone and has been uploaded to Sharepoint at "Execution > FY11 > Program Tracking > Milestones > 2.0 Evidence > PoR-2 > L2s > RTM.P2.01". The models referenced in the report are also stored in the OLCF's HPSS archival storage system in B. Kochunas' user space, as no CASL space has been designated. The code developed and modified to complete this work can be accessed in the CASL repositories.

Tasks to Complete the Milestone:

To complete this milestone CD-Adapco created the STAR-CCM+ model and Michigan created a DeCART model based on the STAR-CCM+ model's geometry and developed a realistic core design. Some code development was required to improve the efficiency of data transfer for coupling DeCART and STAR-CCM+. In the previous interface method all data was transferred using a single file and was adequate for the smaller multi-assembly problems performed in PoR-1 milestones (L1.CASL.Y1.02). However, this method was simply too cumbersome and memory intensive for the full core problem performed in this PoR-2 milestone. In order to complete this task it was also necessary to extend the capability of DeCART to accommodate a jagged core boundary and "off-set" assemblies on the core periphery which are unique to Combustion Engineering (C/E) cores. Details of these improved features are described in the attached report.

Person(s) Responsible for Completing the Milestone:

Brendan Kochunas - University of Michigan
Shane Stimpson - University of Michigan
Thomas Downar - University of Michigan
Robert Brewster - CD-adapco
Emilio Baglietto - CD-adapco

Regards,

Thomas Downar

Attachment: 1. "DeCART/STAR-CCM+ Coupled Simulation of a Quarter-Core C/E Plant".

Consortium for Advanced Simulation of LWRs
Consortium for Advanced Simulation of Light Water Reactors
Bldg. 2040, Room E-170, MS 6290
P.O. Box 2008
Oak Ridge, TN 37831-6290
Email: casl-info@ornl.gov

DeCART/STAR-CCM+ Coupled Simulation of a Quarter-Core C/E Plant

by

Brendan Kochunas, University of Michigan
Thomas Downar, University of Michigan
Robert Brewster, CD-adapco
Emilio Baglietto, CD-adapco

June 30, 2011

Introduction

This report provides details of the work performed during PoR-2 to demonstrate a full-core 3D MOC transport (2D/1D, pin-resolved) capability with single phase CFD T/H coupling. Two calculations were performed. The first was a coupled neutron transport and CFD calculation using DeCART as the neutron physics code and STAR-CCM+ as the thermal hydraulics and heat transfer code. The second calculation was a DeCART stand-alone calculation where T/H feedback was obtained from the simplified internal T/H solver in DeCART. The remainder of this report is divided into six sections. The first two sections provide a detailed overview of the models used by STAR-CCM+ and DeCART. The third section provides an account of software feature enhancements that were implemented as part of this work. The fourth section provides details about the numerical convergence of the coupled calculation. The fifth section reviews the results for each calculation. The last section provides the conclusions drawn from this work and some suggestions for future work.

STAR-CCM+ Model Description

The STAR-CCM+ model was developed by CD-Adapco, and for this initial full core coupled code calculation some simplifications to the model were used to minimize the computational burden. The most important simplification was that the number of mesh in the model was coarser

than typical for CFD. A summary of the element count of the model is provided in Table 1 below.

Table 1 - Summary of CFD Model Elements by Region

Region	Cells	Faces	Vertices
Fluid	124,427,845	357,919,713	138,800,560
Fuel	65,295,300	182,058,660	80,377,234
Fuel Rod Cladding	78,354,360	208,023,144	105,701,568
Guide Tube Water	5,810,175	16,706,395	6,566,014
Guide Tube Cladding	2,582,300	6,422,820	3,922,890
Total	276,469,980	771,130,732	335,368,266

Other simplifications included in the model were to not explicitly model the fuel pellet/clad gap and to treat the water in the guide tubes as solids in order to avoid multiple inlet/outlet boundaries. All of these simplifications will be relaxed in subsequent models which will be used for challenge problem applications.

The STAR-CCM+ model extended below the bottom of the DeCART model in order to represent the part of the assembly below the active fuel and to allow the flow field to develop prior to entering the active fuel regions. The physical models used for the simulation are summarized in Table 2. Default parameters for the all the solvers were used and the polynomial used for computing the fluid density was derived from the steam tables used in the DeCART internal T/H solver. The remainder of the thermophysical properties were set to constants and are given in Table 3. The grid spacers were modeled as porous media, so only their affect on the pressure drop is captured within the model. The system pressure was set to be 2250 psia and the inlet condition is a uniform velocity of 5.278 m/s and the inlet temperature is given as 542.5 °F (283.61 °C). Figure 1 shows the CFD mesh radially for a quarter of an assembly. The exact amount of memory required by STAR-CCM+ at run time is uncertain but it is on the order of hundreds of GB.

Table 2 - STAR-CCM+ Computational Physics Models by Material

Material	STAR-CCM+ Models
Fluid	Liquid Polynomial Density Reynolds-Averaged Navier Stokes Steady Three Dimensional Segregated Flow Segregated Fluid Energy Turbulent K-Epsilon Turbulence Standard K-Epsilon High y+ Wall Treatment
Fuel	Solid Constant Density Steady Three Dimensional Segregated Solid Energy
Fuel Rod & Guide Tube Cladding	Solid Constant Density Steady Three Dimensional Segregated Solid Energy
Guide Tube Water	Solid Constant Density Steady Three Dimensional Segregated Solid Energy

Table 3 - Thermophysical Properties of Materials

Material	Property	Value
Fluid	Dynamic Viscosity [Pa-s]	8.436E-5 Pa-s
	Specific Heat [J/kg-K]	5758.6 J/kg-K
	Thermal Conductivity [W/m-K]	0.54167 W/m-K
	Turbulent Prandtl Number	0.9
	Polynomial Density [kg/m^3]	(100 K ≤ T < 618 K) $\rho = 75505.69389 - (387.111481)T + (0.671649734)T^2 - (3.00608\text{E}-04)T^3$ (618 K ≤ T < 5100 K) $\rho = 594.17$
Fuel	Density [kg/m^3]	10400.0
	Specific Heat [J/kg-K]	300.0
	Thermal Conductivity [W/m-K]	6.0
Clad	Density [kg/m^3]	6500.0
	Specific Heat [J/kg-K]	350.0
	Thermal Conductivity [W/m-K]	17.0
Guide Tube Water	Density [kg/m^3]	781.0
	Specific Heat [J/kg-K]	5950.0
	Thermal Conductivity [W/m-K]	0.547

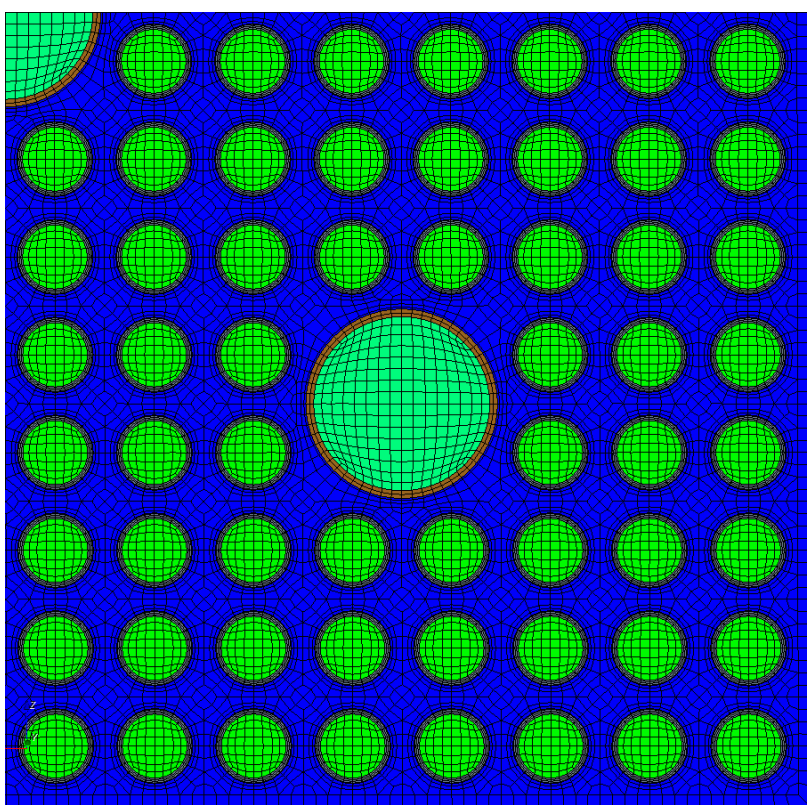

Figure 1 - STAR-CCM+ Mesh for Quarter of a Fuel Assembly

DeCART Model Description

The DeCART model geometry and mesh were based on the STAR-CCM+ model, except that the DeCART model used a radial reflector region which was not modeled in STAR-CCM+. Conversely, STAR-CCM+ modeled an axial reflector region but the axial reflector was not modeled in DeCART. In subsequent models which will be used for challenge problem applications both axial and radial reflector regions will be modeled and coupled in DeCART and STAR-CCM+.

The boundary conditions for the DeCART model were vacuum axially and radially, with the exception of the quarter-core symmetry boundaries which are specular reflective. The axial mesh used in DeCART for the coupled model coincides with the mesh boundaries of the STAR-CCM+ model in order to insure consistency of the mapping and to provide acceptable accuracy of the DeCART 1-D solver. For the stand-alone T/H DeCART model, an equal spaced axial mesh that differs from the coupled model was used in which the total number of planes was the same in neutronics and T/H.

Because of proprietary concerns the core loading pattern and assembly designs was not based on actual startup core. Instead an approximate startup core was designed with an assembly layout shown in Figure 2. The assembly designs including material compositions are shown in Figure 3 through Figure 7. For brevity, the material compositions and detailed geometry information are omitted here, but are included in the DeCART input file. The assembly average power was assumed to be 17.9228 MW. The average assembly mass-flow rate at the inlet was specified as 102.0704 kg/s and derived from the STAR-CCM+ model which used a velocity inlet condition as noted in the previous section. The inlet temperature was assumed to be the same as the STAR-CCM+ model. This core design and model can be treated as non-proprietary.

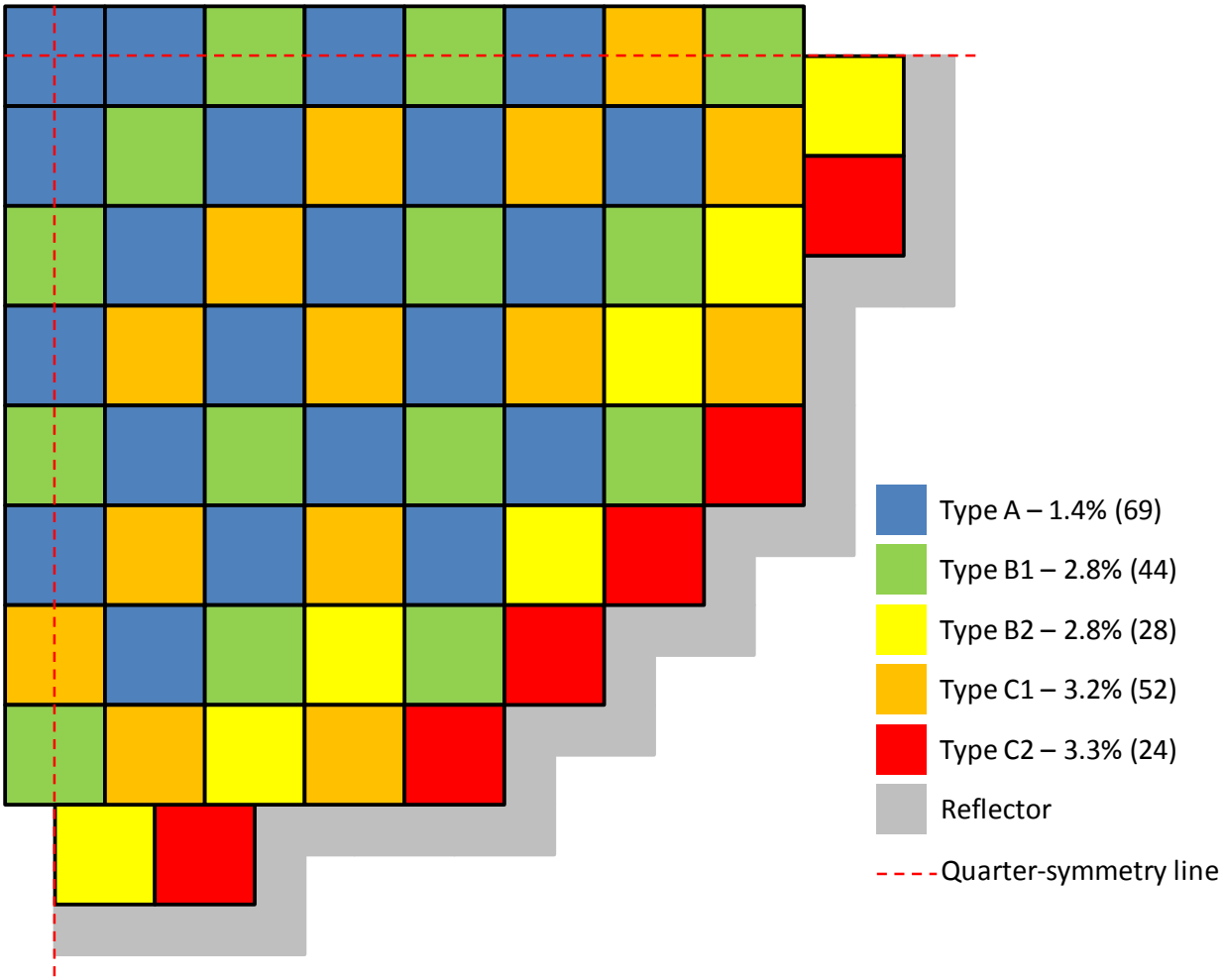

Figure 2 - Core Loading Pattern

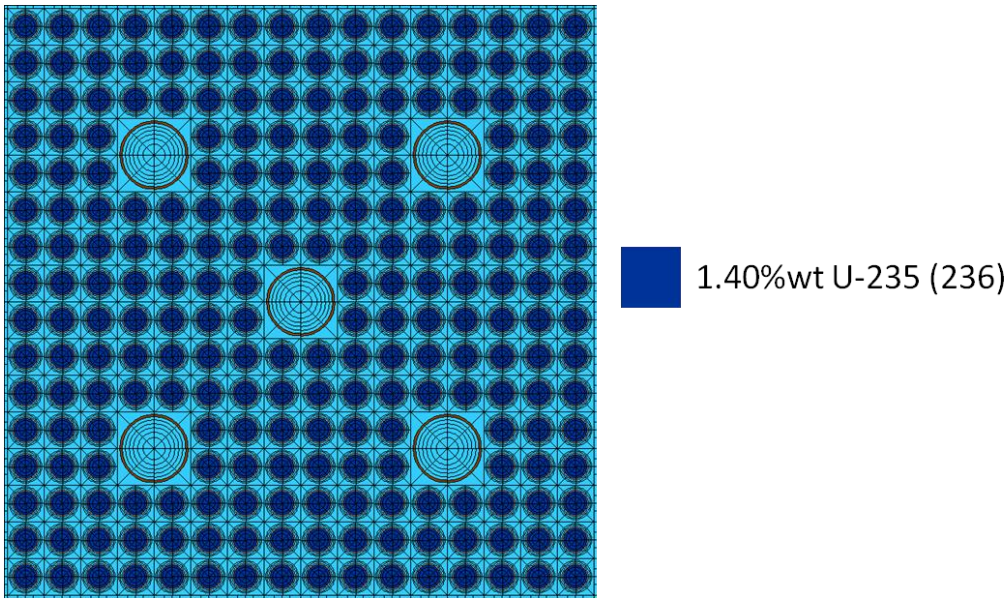

Figure 3 - Type A Assembly Design

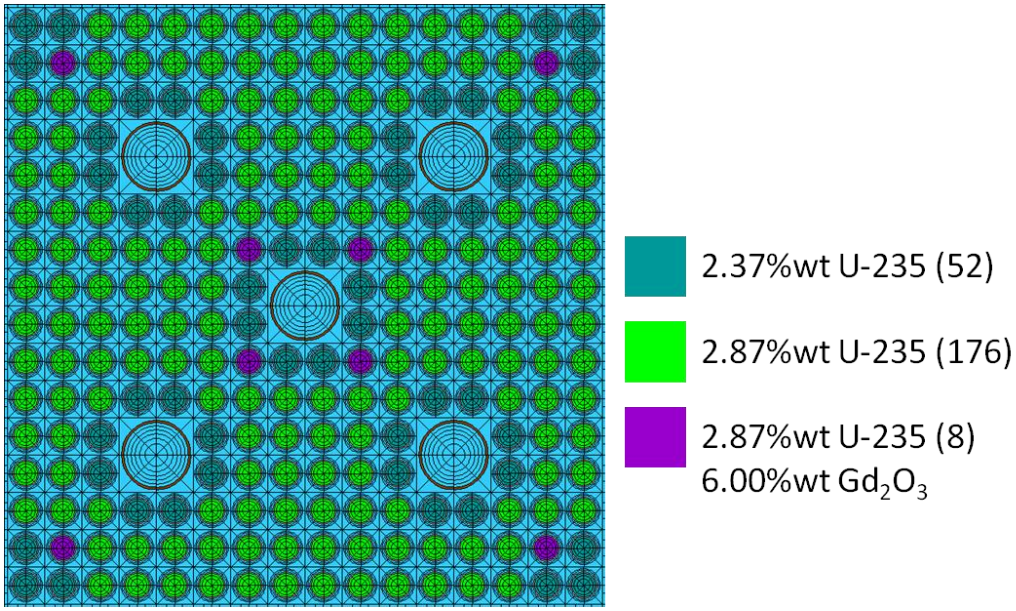

Figure 4 - Type B1 Assembly Design

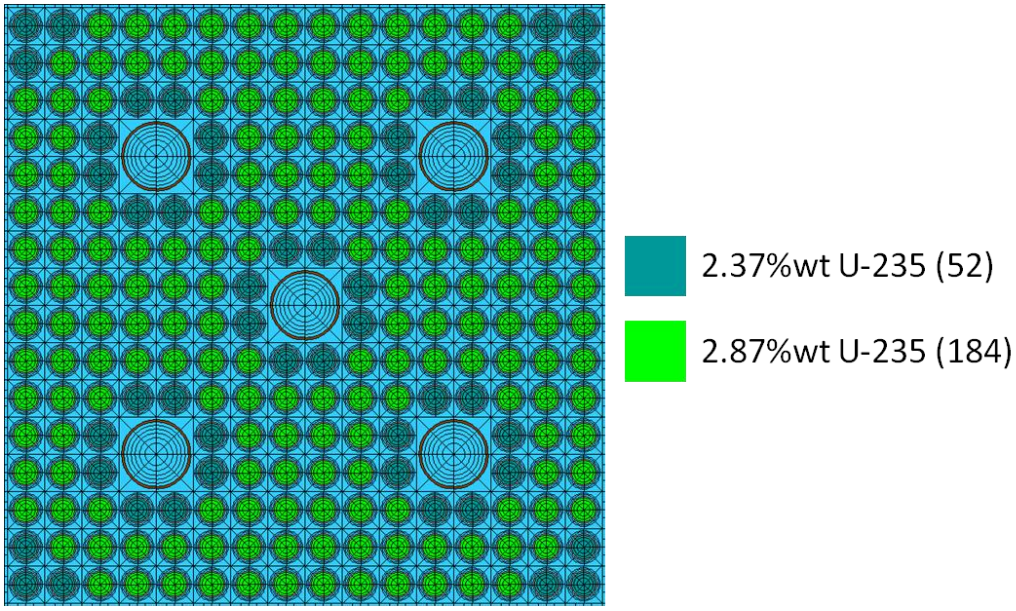

Figure 5 - Type B2 Assembly Design

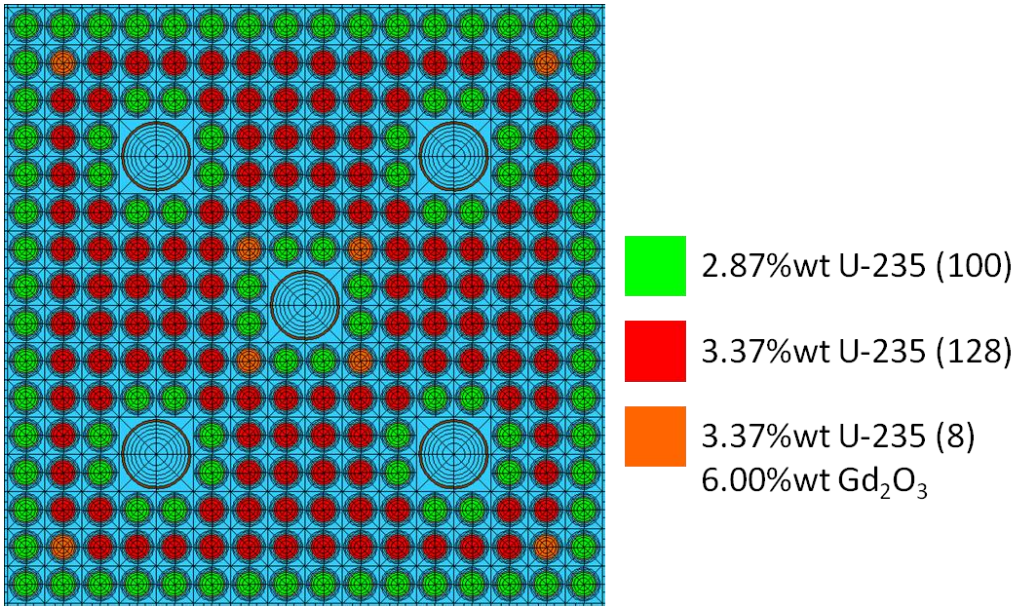

Figure 6 - Type C1 Assembly Design

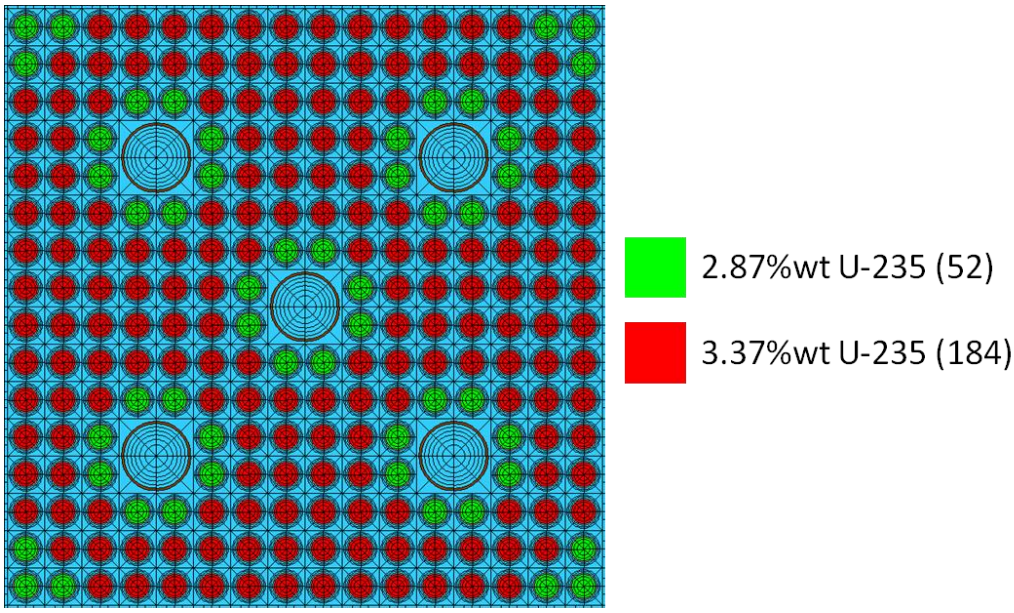

Figure 7 - Type C2 Assembly Design

The cross-sections for DeCART were based on its native 47-group library and the sub-group method was used to perform resonance self-shielding. In order to most closely simulate full power conditions, a critical boron search and an equilibrium xenon concentrations were assumed.

The discretization of the DeCART model used the default ray settings of 0.05 cm spacing with 4 azimuthal and 2 polar angles per quadrant. The convergence criteria was set to 1.E-5, where convergence was measured by the change in k-eff between successive iterations and the 2-norm of the residual of the CMFD linear system. A summary of the key parameters influencing the

computational requirements of DeCART are given in Table 4. During execution,the DeCART model required approximately 600 GB of memory.

Table 4 - Summary of DeCART Discretization

Parameter	Value
Number of Neutron Energy Groups	47
Number of Axial Planes	20
Number of Flat Flux Regions	16,134,160
Number of Uniform Cross Section Regions	2,096,500
Number of Characteristic Ray Segments	765,911,600

Software Feature Enhancements

Some minor software development was required to reduce the computational burden and provide the necessary functionality for this problem. This involved modifications to DeCART and also within the coupling interface of DeCART and STAR-CCM+. For DeCART many of the improvements were to enable features that already existed in the code, but only worked for a limited set of problems. The feature improvements included improving the internal T/H solver to work correctly for the geometry used by the C/E assembly designs which required the use of quarter circle pin geometry. Also modifications were made to the assembly modular ray tracing which was necessary to model the inter-assembly gap. Also, model required the development of a re-entrant boundary condition for the ray tracing as depicted in Figure 8.

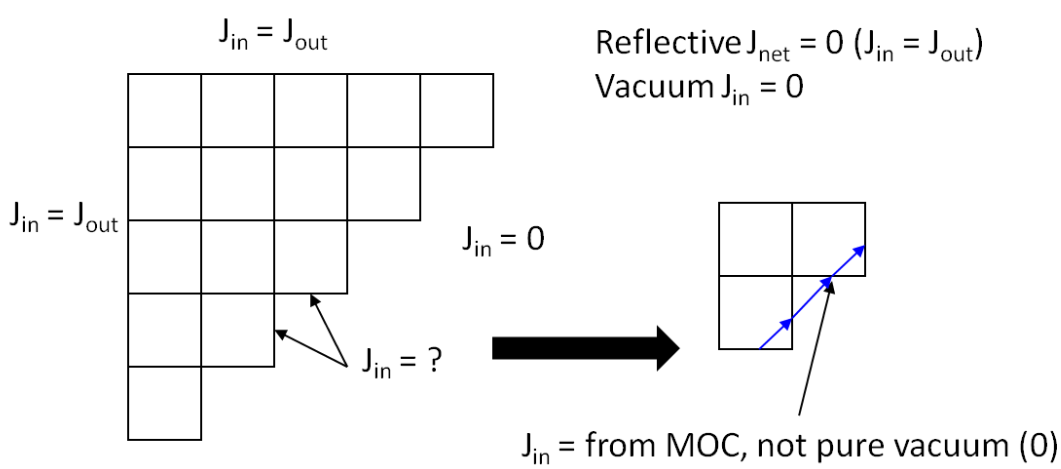

Figure 8 - Re-entrant Boundary Condition

In order to improve the efficiency of the data transfer between the codes, a parallel file I/O was implemented. This required some modifications in DeCART since previously, this feature worked for coupling to STAR-CD, but not STAR-CCM+. It also required a significant amount of work to develop the user-coding for STAR-CCM+. The essential feature of the parallel file I/O is to enable each STAR-CCM+ process to write its own files with all geometry and solution

data required for transfer. DeCART then processes this data and performs the necessary mapping to the appropriate STAR-CCM+ process. When DeCART writes a power distribution it writes the necessary data to a new set of files, one for each STAR-CCM+ process.

One additional consideration was to account for STAR-CCM+ “halo” cells. The mapping algorithm requires that DeCART map only the real cells on each process thereby preventing the same cell from being counted more than once if it is a halo cell on other processors. This insures that DeCART maps only the solution for the real cells onto its domain, but it also means that it prints only the power for each real CFD cell. STAR-CCM+ needs the data for the halo cells on each domain in order to calculate the correct power. Therefore an additional capability was added to the user coding in which STAR-CCM+ was enabled to communicate with itself to determine what other processes have the real cells for each processes halo cells. The communication of the STAR-CCM+ processes was enabled using MPI. However, it should be noted that because STAR-CCM+ loads the user code library as a dynamically linked library the MPI library that is linked to the user-code must be the same as the one used by STAR-CCM+ at run time.

Calculation Details

The calculations were performed primarily on the NCCS machine Frost since it had much less usage than the target platform Jaguar . There was rarely any wait time on Frost before a job was initiated after it was submitted to the queue. This was in contrast to Jaguar where the wait time was often on the order of days. Jaguar also experienced several unscheduled outages, usually at least one per day. Additionally, the current computational methods used by DeCART and STAR-CCM+ are more suitable for Frost since they do not scale to 100,000's of processors typical of Jaguar applications. However, Jaguar was used for some of the STAR-CCM+ model setup and to perform some of the coupled calculations. Additional details on this are given in the section on Computational Performance.

For most applications, DeCART was run using 20 nodes and 4 processors on each node for a total of 80 processors. STAR-CCM+ was run with 32 nodes and 8 processors on each node, for a total of 256 processors. The coupled calculation was performed as a series of jobs since some of the Software Feature Enhancements developed in the work are not yet implemented into VERA. As a result of running the calculation as a series of jobs the method by which the coupled solution was obtained was equivalent to a Fixed-Point Gauss-Seidel iteration as illustrated in Figure 9. The data transfer between the codes used parallel file I/O described previously in which each STAR-CCM+ process writes its own file and DeCART processes these files in parallel.

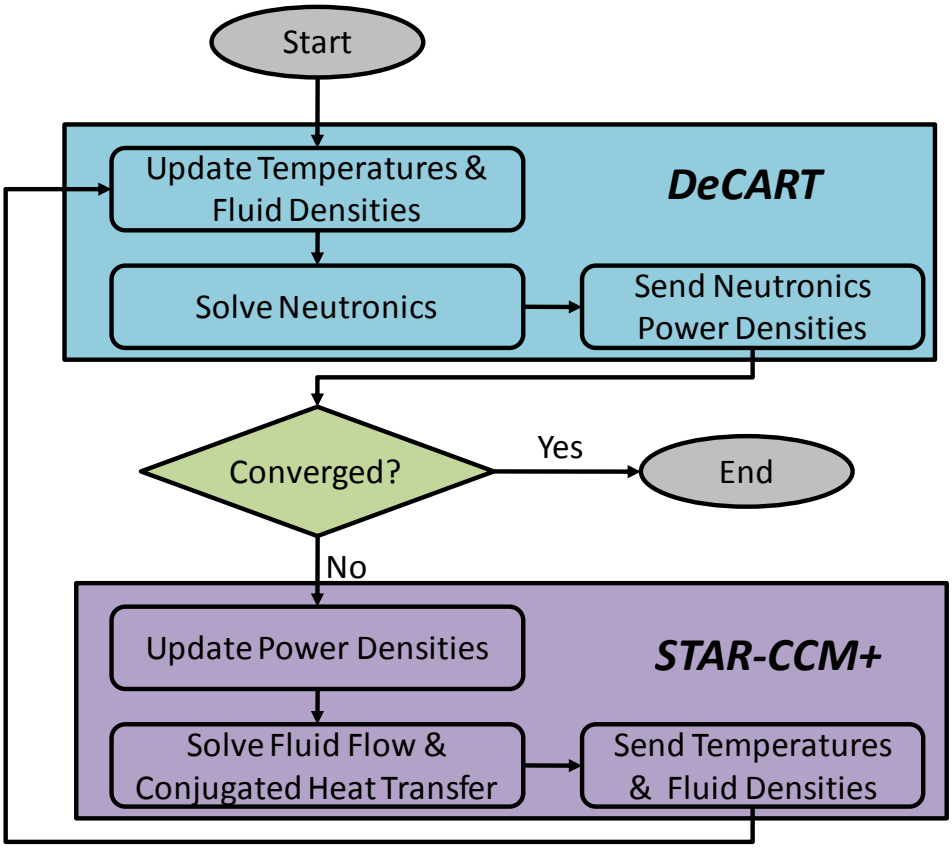

Figure 9 - Coupled Fixed Point Seidel Iteration

Results

Two separate sets of calculations were performed, first a DeCART standalone calculation with internal T/H, and then the coupled STAR-CCM+/DeCART calculation. The standalone calculation was used solely to provide an independent check on the STAR-CCM+ result and a comparison of the CFD with a lower order T/H solution that is typical of the methods currently used in the industry. The standalone solution was not used to provide an initial guess for the coupled code calculation.

DeCART Stand-alone Results

The convergence of the DeCART standalone calculation is shown in Figure 10. Convergence was achieved when the 2-norm of the CMFD residual and the difference in k-eff between successive iterations was less than 1.E-5. As indicated, for this problem the eigenvalue converges slightly faster than the 2-norm of the CMFD residual.

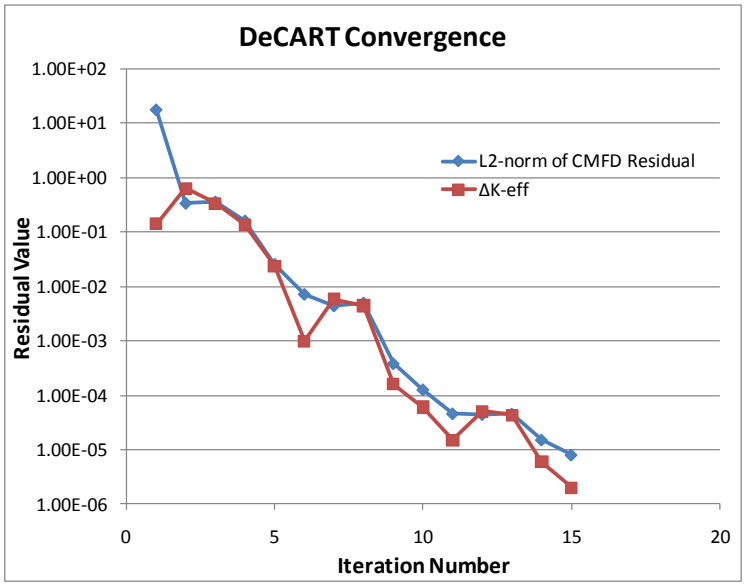

Figure 10 - Convergence of the DeCART Stand-alone Calculation

A summary of some of the global quantities of interest is provided in Table 5. It is noted that the critical boron concentration is a few 100 ppm lower than what may be typical at beginning of cycle (BOC) for an operating PWR with an 18 month cycle. This is most likely the result of using a vacuum boundary condition for the axial direction which results in an over-estimate of the core leakage and consequently, the under-prediction of the critical boron concentration. It is also noted that the maximum centerline fuel temperature is somewhat low compared with typical values, however, the maximum pellet averaged fuel temperature is reasonably close to an expected value at operating conditions. The F_q factor is somewhat high, but not far from what would be an acceptable design limit. Nonetheless, the core design here is more than adequate for the demonstration of a coupled CFD and MOC capability.

Table 5 - Stand-alone Calculation Solution Global Quantities

Global Parameter	Value
Critical Boron Concentration	967.98 ppm
Core Average Coolant Density	0.72403 g/cc
Core Average Fuel Temperature	542.19 °C
Average Outlet Temperature	315.41 °C
Quarter Core Total Power	972.312 MW
Maximum Pin Averaged Fuel Temperature	865.97 °C
Maximum Centerline Fuel Temperature[1]	1162.6 °C
Maximum Relative Pin Peaking Factor (F_q)	2.3148
Maximum Radial Pin Peaking factor (F_{xy})	1.5859
Maximum Axial Pin Peaking factor (F_z)	1.4470

[1] - This is computed based on the analytic solution of the heat equation derived from a 1-D cylinder with a volumetric heat source, so it represents the value at the true centerline.

The calculated relative power distributions in the core is shown in Figure 11 and Figure 12. Figure 11 shows the axially integrated radial pin power distribution for the southwest quadrant of the core, and Figure 12 is the radially integrated 1-D axial power shape. The peak pin location is located in the ninth plane up from the inlet at a height of approximately 167.035 cm, and its x-y position is annotated in Figure 11.

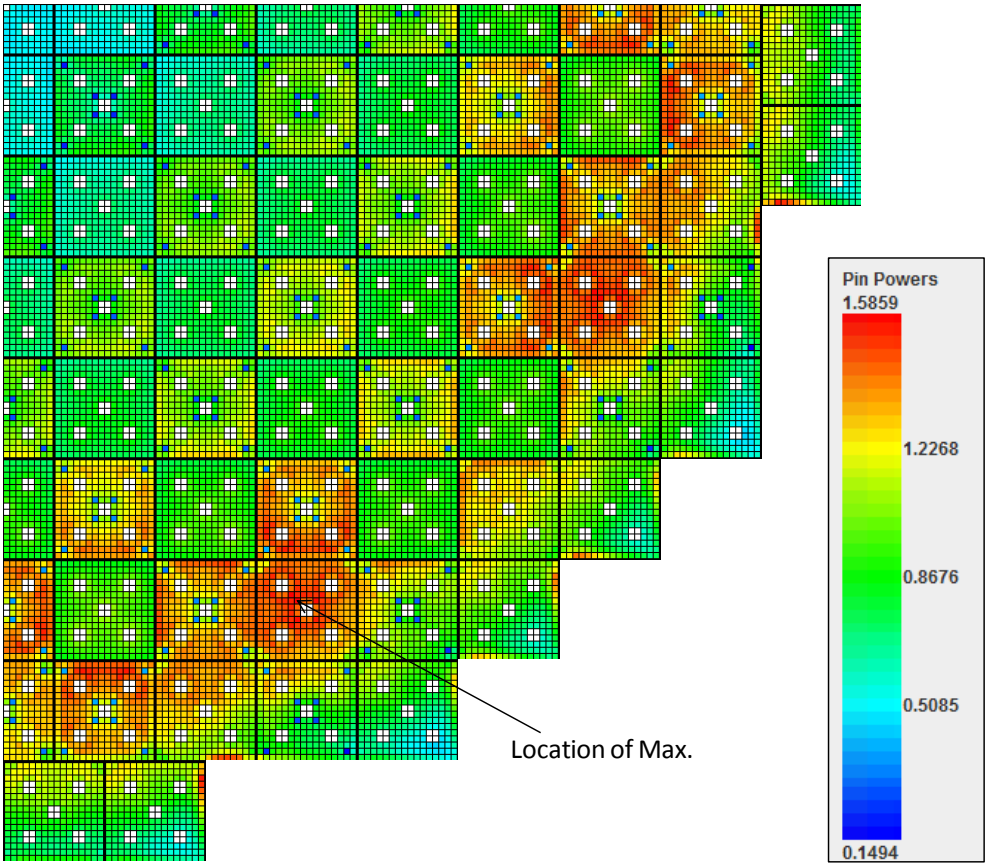

Figure 11 - Stand-alone Calculation Relative Pin Power Distribution

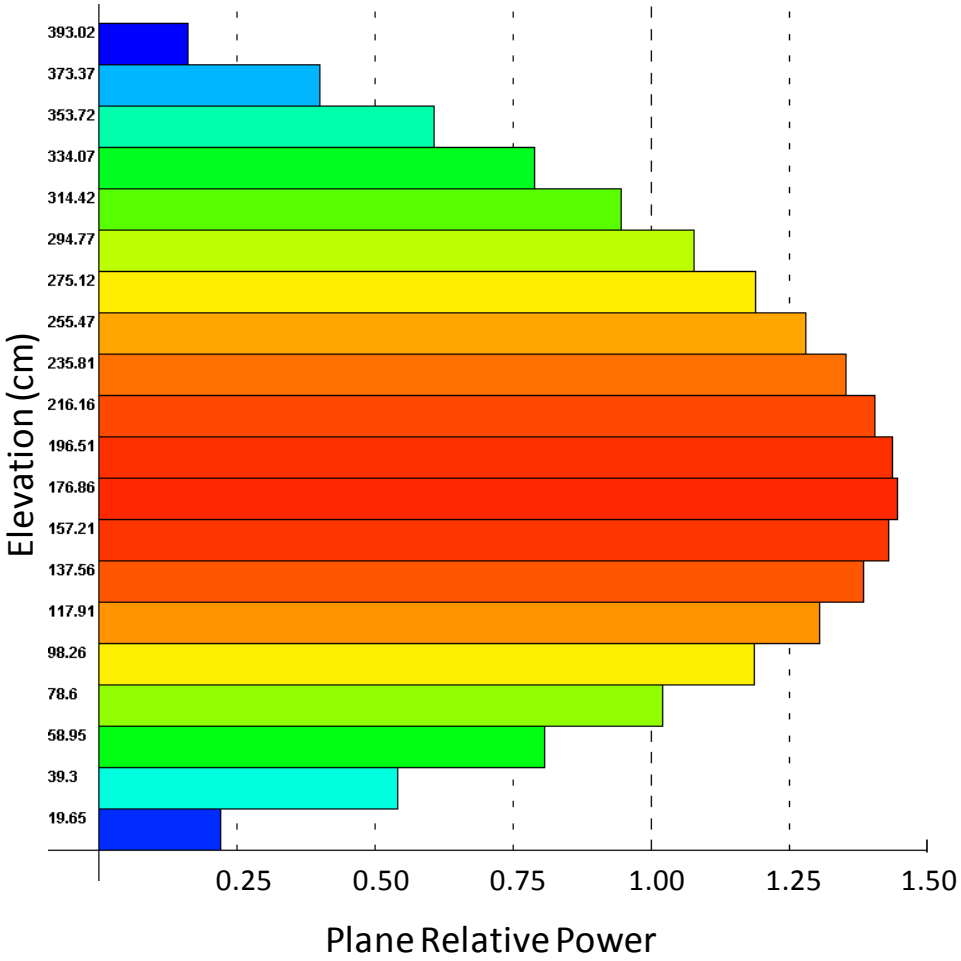

Figure 12 - Stand-alone Calculation 1-D Relative Axial Power Distribution

Coupled Code Results

The convergence of the coupled STAR-CCM+ and DeCART calculation is shown in Figure 13. Similar to the standalone DeCART calculation, convergence was assumed when the difference in subsequent iterations of all the residuals was less than 1.E-5. A large jumps in the residuals occur when there are data exchanges and the power distribution is updated in STAR-CCM+. The "Tke" and "Tdr" in the legend correspond to the turbulence kinetic energy and dissipation rate, respectively.

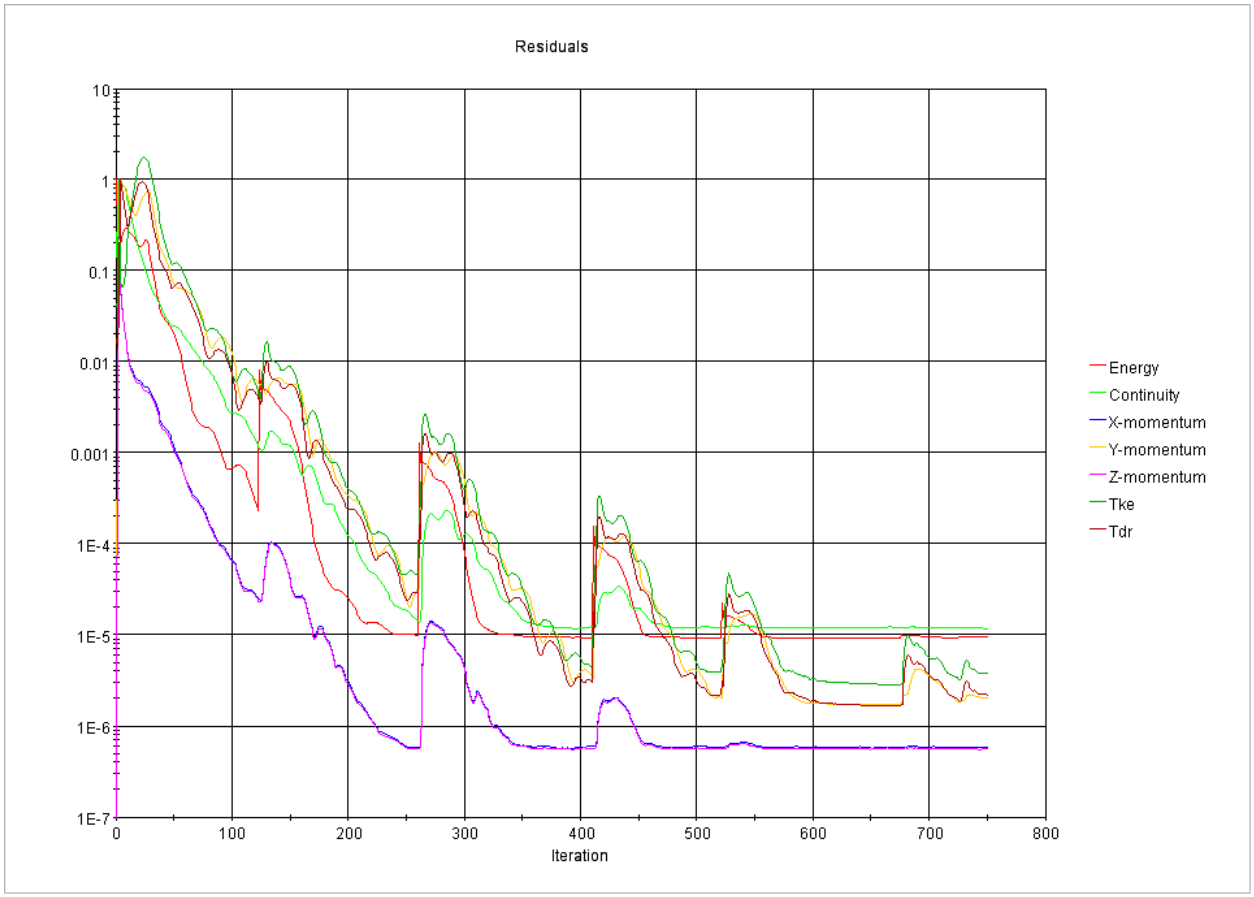

Figure 13 - Coupled Calculation Convergence

A summary of the global quantities of interest from the coupled calculation is shown in Table 6. The predicted critical boron concentration is somewhat higher to the stand-alone DeCART simulation and the core average fuel temperature is notably lower than the stand-alone results. The likely reasons for these differences are the fidelity of the heat transfer calculation which will be discussed in the next section.

It is also worth noting that in the coupled code calculation there are slight differences in the core average temperatures computed in STAR-CCM+ and DeCART. In Table 6, for the average fuel temperature the first value is the one computed by STAR-CCM+, and the second value in parenthesis is the one computed by DeCART. The reason that they are not identical is due primarily to slight differences in the mesh mapping since the mesh between the two codes are not exactly conformal. The mesh mapping differences also results in differences in the quarter core total power computed by DeCART and STAR-CCM+. The total power computed by DeCART in the coupled calculation is identical to the value computed in the standalone calculation which was shown in Table 5. The reason the STAR-CCM+ and DeCART power calculations differ by 0.48% is because of mesh mapping. Methods for resolving this will be addressed in future coupled code calculations.

Table 6 - Coupled Calculation Solution Global Quantities

Global Parameter	Value
Critical Boron Concentration	982.48 ppm
Core Average Coolant Density	0.72945 g/cc
Core Average Fuel Temperature[1]	463.52 °C (464.89 °C)
Average Outlet Temperature	316.36 °C
Quarter Core Total Power[2]	967.618 MW
Maximum Fuel Temperature[3]	975.06 °C
Maximum Relative Pin Peaking Factor (F_q)	2.3595
Maximum Radial Pin Peaking factor (F_{xy})	1.6012
Maximum Axial Pin Peaking factor (F_z)	1.4608

[1] - The value is computed by STAR-CCM+, the value in parentheses is the value computed by DeCART.
[2] - This value is computed by STAR-CCM+
[3] - This is the maximum value of all STAR-CCM+ cells, which differs from the temperature at the true centerline of a cylinder as calculated by DeCART.

The calculated relative power distributions computed by DeCART is shown in Figure 14 and Figure 15. Figure 14 is the axially integrated radial pin power distribution, and Figure 15 is the radially integrated 1-D axial power shape. The peak pin location is located in the eighth plane up from the inlet at approximately 166.21 cm, and its x-y position is annotated in Figure 14.

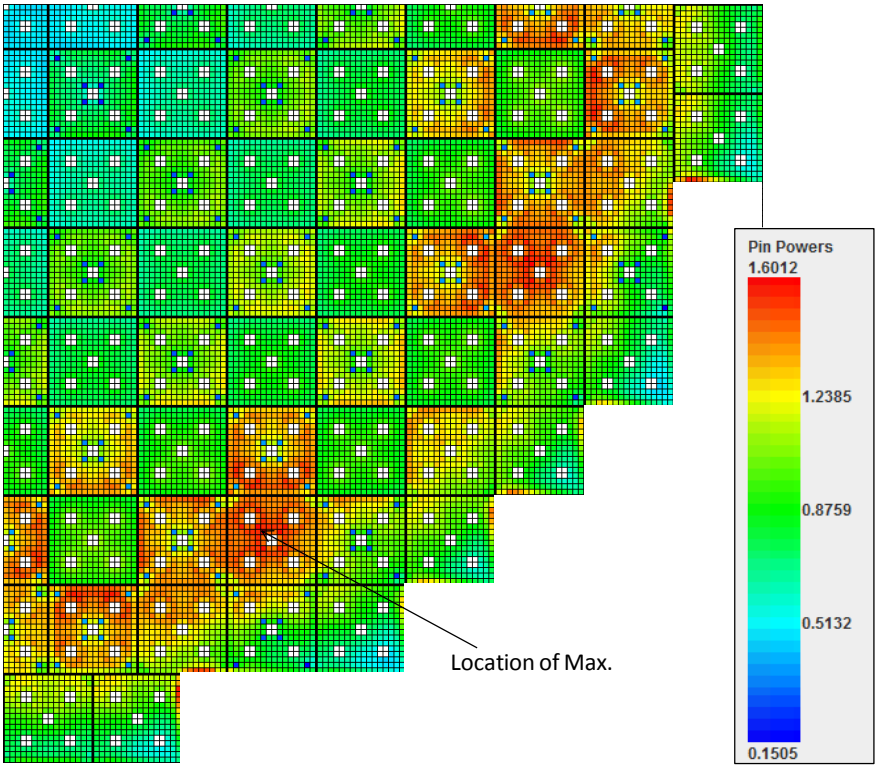

Figure 14 - Coupled STAR-CCM+/DeCART Relative Pin Power Distribution

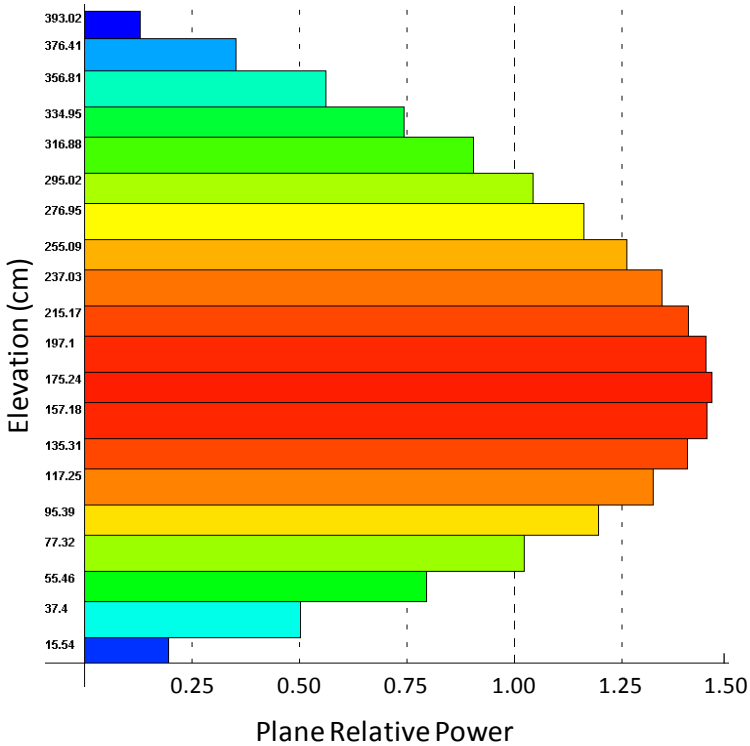

Figure 15 - Coupled STAR-CCM+/DeCART 1-D Relative Axial Power Distribution

Comparison of Standalone and Coupled Results

A comparison of the global quantities from the DeCART Standalone results summarized in Table 5 and DeCART/STAR-CCM+ results in Table 6 are given in Table 7. The difference is computed as the stand-alone result subtracted from the coupled result. The relative differences are also given in parentheses and are computed with the coupled result as the reference value.

Table 7 - Comparison of Global Quantities

Global Parameter	Difference
Critical Boron Concentration	-14.5 ppm (-1.48%)
Core Average Coolant Density	-0.00545 g/cc (-0.75%)
Core Average Fuel Temperature	78.67 °C (16.97%)
Average Outlet Temperature	-0.95 °C (-0.30%)
Quarter Core Total Power	4.694 MW (0.49%)
Maximum Relative Pin Peaking Factor (F_q)	-0.0447 (-1.89%)
Maximum Radial Pin Peaking factor (F_{xy})	-0.0153 (-0.95%)
Maximum Axial Pin Peaking factor (F_z)	-0.0138 (-0.94%)

A comparison of these parameters provides several preliminary insights about the impact of higher fidelity temperature-fluids feedback on the coupled field solution. The fuel temperature calculation performed in DeCART standalone is typical of those used in most reactor analysis

codes and is based on a 1-D solution of the heat conduction equation with a heat transfer coefficient based on the Dittus-Boelter correlation. Conversely, the CFD calculation is 3D and based on conjugate heat transfer. As indicated in the Table 7, higher peaking factors are predicted by the coupled model which would indicate the stand-alone solution may be less conservative. This effect is consistent with the higher temperatures and stronger T/H feedback in the stand-alone simulation which would result in slightly flatter powers and less peaking. A likely reason for the higher fuel temperature would be the difference in heat transfer between the simulations since they are both using the same thermal conductivities. Future work will include a more thorough analysis of these differences and the impact on key safety parameters.

A summary of the differences in the power distributions between the standalone and coupled simulation is shown in Table 8. Three measures of the difference for four predicted quantities are provided in the Table. Plots of the distributions of the solution differences for the predicted axially integrated pin powers and radially integrated 1-D axial power are given in Figure 16 and Figure 17, respectively. A few things worth noting in Figure 16 are that there is an obvious tilt to the error, where the high power regions are under-predicted by the stand-alone calculation compared with the coupled calculation, and the low power regions are over predicted by the stand-alone compared with the coupled solution. This distribution is also consistent with the stand-alone model having a stronger doppler feedback which is likely the case given the higher average fuel temperatures. In Figure 17 the differences are due in part to the inconsistent axial meshing and probably also as a result of different predicted shapes in the axial fluid density; the lowest power regions having the highest relative error.

Table 8 - Summary of Select Differences of Solution Field

Predicted value	Difference Type	Value
Axially Integrated Relative Pin Power	Maximum Absolute Difference	0.0242
	Maximum Relative Difference (%)	3.37
	RMS (%)	1.12
Radially Integrated 1-D Relative Axial Power	Maximum Absolute Difference	0.1887
	Maximum Relative Difference (%)	60.22
	RMS (%)	18.29
MOC Region Power Density	Maximum Absolute Diff. (W/m^3)	2.9304E+07
	Maximum Relative Difference (%)	28.84
	RMS (%)	7.80
MOC Region Temperature	Maximum Absolute Diff. (°K)	229.01
	Maximum Relative Difference (%)	29.61
	RMS (%)	7.45

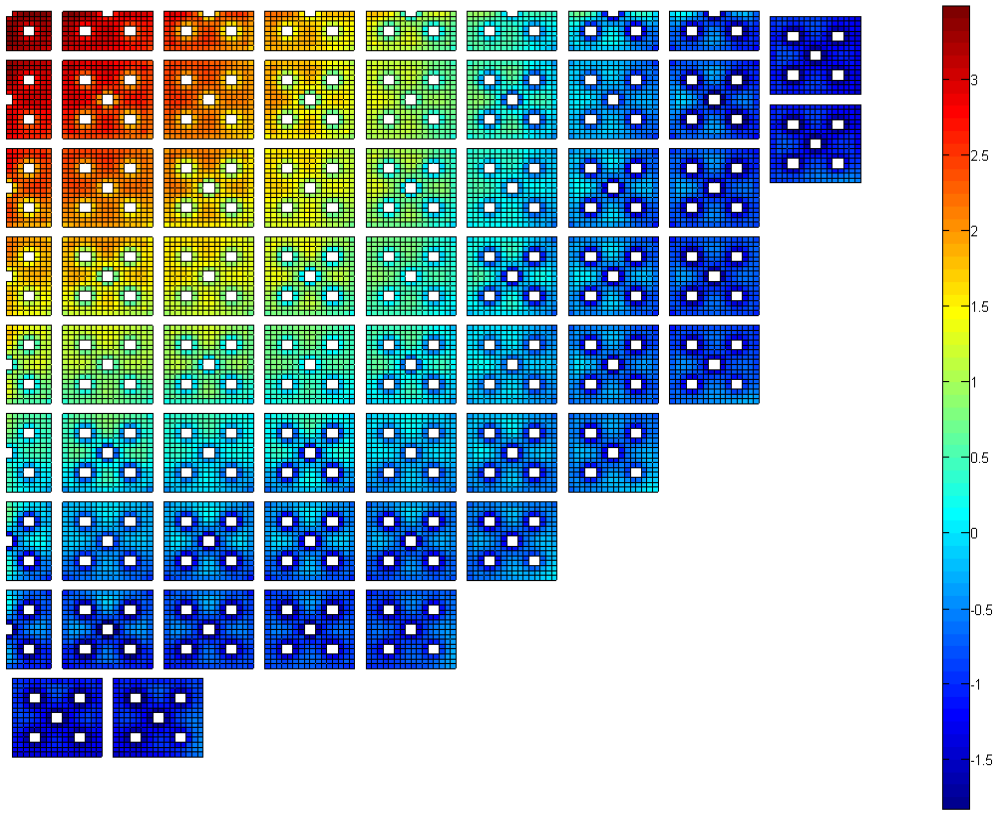

Figure 16 - Relative Difference (%) of Axially Integrated Relative Pin Power Distribution

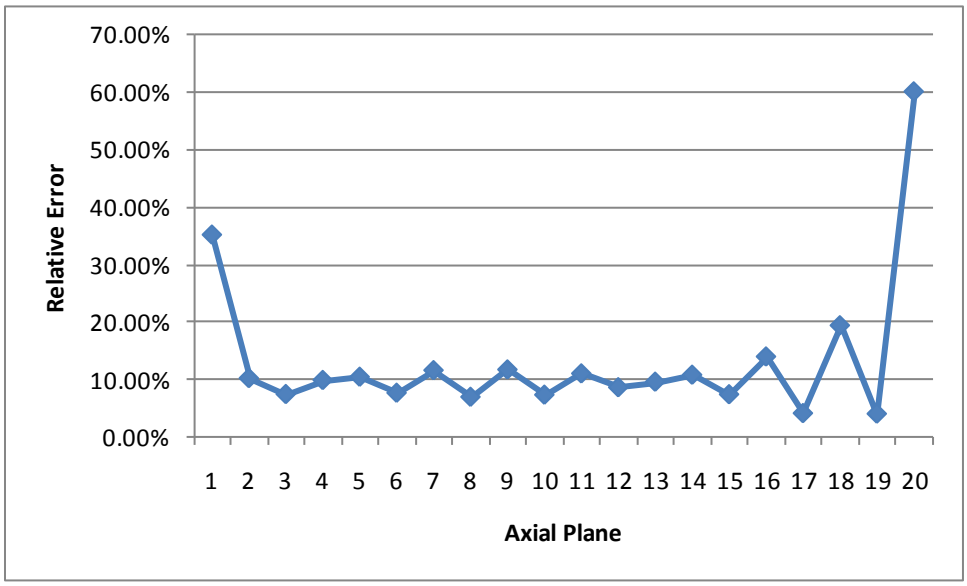

Figure 17 - Relative Difference in 1-D Axial Power Distribution

Computational Performance

For the DeCART stand-alone calculation, the overall run time was 92 minutes and DeCART converged on the 17th iteration. The coupled solution required 6 total fixed point iterations. In the coupled calculation for each fixed point iteration DeCART would run for approximately 105 minutes. The STAR-CCM+, the solution was not re-initialized at each data exchange so the number of iterations within STAR-CCM+ to converge varied at each fixed point iteration. Consequently, the time STAR-CCM+ required for each fixed point iteration decreased as the number of fixed point iterations increased. Each STAR-CCM+ iteration required approximately 2.5 minutes on Frost. A total of 750 STAR-CCM+ iterations were required to converge the coupled solution. Table 9 below shows a breakdown of the estimated computational times and CPU hour requirements for each calculation component. Figure 18 shows the CPU hour requirements for each component task for the coupled simulation.

Table 9 - Times of different calculation components

Calculation Component	Est. Total Time (min)	CPU Hours
DeCART Fixed Point Iter.	105.57	140.76
STAR-CCM+ Fixed Point Iter.	399.00	1702.40
DeCART Total (Coupled)	633.43	844.58
STAR-CCM+ Total (Coupled)	1995.00	8512.00
Total (Coupled)	2628.43	9356.58
DeCART Total (Stand-alone)	86.59	115.46

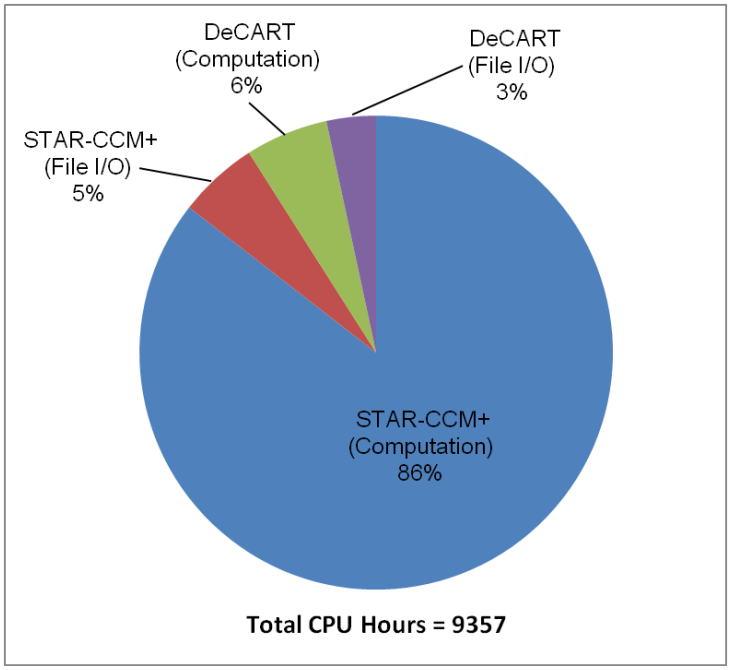

Figure 18 - CPU Hour Requirements of Coupled Simulation by Component Task

Some additional comments are worth noting about the calculation with respect to STAR-CCM+ and the Jaguar and Frost machines. In running this calculation, iterations were attempted on Jaguar but were observed to take ~20 minutes per iteration compared to 2.5 minutes on Frost. It is unclear why this should be the case, but the reasons will be studied in future work. Furthermore, problems were also encountered running STAR-CCM+ on Frost. It was observed that some jobs would fail or hang while others did not, with the only difference between jobs that worked and those that did not work being the nodes on Frost that were used. This would indicate some problem between STAR-CCM+ and Frost's architecture and that not all nodes, or communication between nodes on Frost is equivalent. Some STAR-CCM+ operations, such as partitioning the model, also seemed to fail on Frost, but worked fine on Jaguar. The reason for this behavior is also unclear and will studied in future work.

Conclusions and Suggested Future Work

The full core coupled DeCART neutronics and single phase T/H was performed in this milestone. A standalone calculation was performed with DeCART internal TH in order to provide a basis for comparison. The computational requirements of these calculations were reported and it should be noted that the coupled calculation requires almost 100x the computational resources compared to the stand-alone simulation. The majority of this additional burden is from the CFD code, indicating the importance of a CFD code that scales well. In terms of predicted quantities there were some significant differences that require further investigation. The most important of these were the impact on the fuel temperature because of differences in the heat transfer at the fluid/solid interface of a fuel rod. Initial results suggest that the more sophisticated 3D, conjugate heat transfer used in the CFD code may provide a more conservative temperature and power distribution than the lower order solution based on the Dittus-Boelter heat transfer coefficient. A more thorough study is recommended for future work which should include a detailed comparison of not just the heat transfer coefficient but also the fluid heat capacity in order to resolve differences in average outlet temperature.

Other recommendations for future work would include the development of methods to initialize the STAR-CCM+ solution in a coupled calculation with a DeCART stand-alone result. The software feature enhancements described here should also be implemented into the coupling interface in LIME. There are still some outstanding questions with regards to the axial meshing, and methods should be developed to perform and normalize the calculations with consistent axial mesh in DeCART and CCM+. Additionally, grid refinement studies for both codes are suggested. Regarding the computational performance, scaling studies on the CFD model should be performed, since it is likely that more processors could be used to reduce the STAR-CCM+ run time.